Chapter 5
The Multiwavelength UV/Vis Detector: New Possibilities with an Added Spectral Dimension

Engin Karabudak and Helmut Cölfen

Abstract The multiwavelength (MWL) detector is a new type of absorption detector for AUC. The commercial absorption detector of the Beckman Coulter XL-A AUC can only handle a single wavelength per scan with the possibility to scan at maximum 3 wavelengths, whereas MWL-AUC can handle all the wavelengths in the UV/Vis region at one time. The result is impressive since now a full spectral dimension is added to each single scan. In this chapter, we are explaining development history, instrumentation, and future perspective of MWL-AUC.

Keywords Analytical ultracentrifuge • UV/Vis spectroscopy • Separation • Instrumentation • Detector • Proteins • Multiwavelength detector • Online detection

5.1 Introduction

Analytical ultracentrifugation (AUC) allows the determination of important physicochemical quantities like sedimentation and diffusion coefficients, molar mass, size and shape, as well as the stoichiometries and equilibrium constants of interacting systems. Its power is in its ability to fractionate the sample, enabling the investigation even of most complex mixtures. However, every AUC experiment requires the detection of the relevant analytes, which in turn calls for a number of parallel available optical detectors to maximize the range of molecules.

Traditionally, AUC is equipped with refractive index (Schlieren and Rayleigh interference) as well as UV/Vis detectors. The latter enables the detection of the radial concentration profile at one wavelength. The commercially available Beckman Coulter XL-I is equipped with UV/Vis and Rayleigh interference optics.

E. Karabudak
Chemistry Department, Izmir Institute of Technology, TR-35430 Izmir, Turkey

H. Cölfen (✉)
Department of Chemistry, University of Konstanz, Universitätsstr. 10, D-78457 Constance, Germany
e-mail: Helmut.Coelfen@uni-konstanz.de

S. Uchiyama et al. (eds.), *Analytical Ultracentrifugation*,
DOI 10.1007/978-4-431-55985-6_5

A fluorescence detector also is available as a retrofit for this instrument (MacGregor et al. 2004). For nanoparticles, special turbidity detectors were developed, which allow the detection of very broad particle size distributions using a rotor velocity profile (gravitational sweep technique) (Müller 1989; Mächtle 1999). Fluorescence and turbidity detectors extend the range of applications for AUC considerably. However, especially in the field of nanoparticles, size-dependent optical properties are observed, such as bandgap absorbance for semiconductors or the plasmon resonance for metal nanoparticles. The investigation of such samples would benefit very much from the detection of UV/Vis absorption spectra while the sample is fractionated by the ultracentrifugal field. The same is true for mixtures of samples with different chromophores, regardless if nanoparticle or (bio)polymer. This was the scientific motivation for the development of a multiwavelength (MWL)[1] UV/Vis detector, which allows the detection of a full spectrum instead of a single wavelength.

5.2 The Multiwavelength Detector

The multiwavelength (MWL) detector is a new type of absorption detector for AUC. The commercial absorption detector of the Beckman Coulter XL-A AUC can only handle a single wavelength per scan with the possibility to scan at maximum 3 wavelengths, whereas MWL-AUC can handle all the wavelengths in the UV/Vis region at one time. The result is impressive since now a full-spectral dimension is added to each single scan as shown in Fig. 5.1. Each component in multicomponent samples can thus easily be tracked by MWL-AUC. Data of MWL-AUC are conveniently observed as a movie of sedimentation that includes all

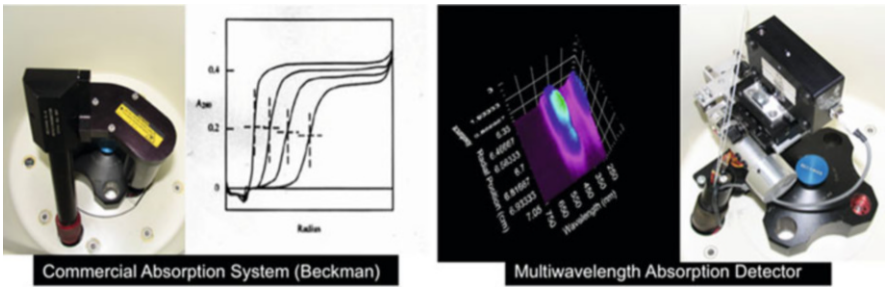

Fig. 5.1 Commercial UV/Vis absorption detector of the Beckman Coulter XL-I and the multiwavelength absorption detector (Reproduced from Karabudak (2009) with permission)

[1]Please note that besides MWL, also the abbreviation MWA for multiwavelength absorption detector is used in the literature. Both abbreviations are equivalent.

Table 5.1 Comparison of commercial XL-A and open-source MWL-AUC second-generation detector

	Commercial absorption system (Beckman)	Multiwavelength detector
Data	Single wavelength per radial point	Full UV/Vis spectrum per radial point
Technology	Photomultiplier tube (1990)	CCD
Cell scan time	1.5 min with 50 μm steps	45 s with 50 μm steps
Minimum motor step size	10 μm	100 nm
Software	Commercial	Open source

the wavelengths of the UV/Vis region, which is an advantage for multicomponent samples.

It is important to compare MWL-AUC and the commercial XL-A AUC in order to explain the novelty of MWL-AUC. First of all, MWL-AUC costs about $50.000 including the basis preparative ultracentrifuge, whereas the commercial XL-A ultracentrifuge costs about a factor of 10 more. In addition, MWL-AUC is an open-source project in the framework of the open AUC project (Coelfen et al. 2010). Nothing is confidential and anyone can get the designs and can build his own detector by downloading the construction plans for free from the open AUC website (http://wiki.bcf2.uthscsa.edu/openAUC/wiki/WikiStart). Its detector technology is also different; MWL-AUC is using CCD technology, whereas the XL-A uses a photomultiplier tube. The CCD technology allows for a very fast readout of the CCD pixels in the ms time range yielding a full UV/Vis spectrum in ms. One single wavelength radial scan takes about 1.5 min in the XL-A and the full wavelength scan about 45 s in the MWL-AUC. The minimum detector step size is less than 1 μm in MWL-AUC and 10 μm in the XL-A. The comparison can be seen in Table 5.1.

In this chapter, we will present the history of the development, optical parts, mechanical parts, software, and electronics of MWL-AUC, and we will give examples of chemical, biological, and industrial applications of MWL-AUC.

5.3 History of MWL-AUC Development

The commercial Beckman Coulter Optima XL-A has an optical system using a Xenon flash lamp with a maximum flash frequency of 100 Hz. White light from this lamp is passed to a toroidal diffraction grating and the system sends the now monochromatic light with pre-selected wavelength via the measurement cell to a photomultiplier tube (PMT) (Giebeler 1992). This optical setup is based on the 1990 technology. Technological developments in the last two decades decreased the price of spectrometers, counter cards, analog to digital converters, and other computer-based technologies significantly. In addition, CCD technology became

broadly commercially available. All these new, cheaper, faster, and more precise technologies do not exist in the commercial XL-I AUC.

MWL-AUC was developed as a cooperation project AUC 2004 with BASF SE in the Cölfen lab at the Max Planck Institute of Colloids and Interfaces in Potsdam, Germany, between 2002 and 2009. With the agreement of BASF SE, the detector could be made open source (http://wiki.bcf2.uthscsa.edu/openAUC/wiki/WikiStart). Throughout the years, two different generations of MWL detectors were developed which are described below. The important characteristic of the two detector generations is that they are based on optical UV/Vis fibers which are prone to intensity decrease in the important UV range due to fiber bending and chemical reactions caused by high-energy UV light (fiber solarization). A third-generation MWL optics has been developed by Spin Analytical for the new centrifugal fluid analyzer (CFA) generation of AUC, which will be soon available commercially. This MWL detector is based on a mirror optics, thus eliminating chromatic aberration and, more importantly, avoiding the use of optical fibers (Laue and Austin in press).

5.3.1 First-Generation MWL Detectors

The first-generation MWL was developed on the basis of feeding the light into the AUC vacuum chamber and also feeding it out again to the spectrometer after it has passed the measurement cell. The design is shown in Fig. 5.2. The light from a Xenon flash lamp was coupled into the optical fiber, which had a diameter of 600 μm in order to provide as much light as possible at the detector. However, the large fiber diameter resulted in poor spatial resolution. The light exiting the fiber was collimated to a parallel light beam[2] and then reflected by 90° via a prism or mirror and then passed the cell (Fig. 5.2 left). Then the light was collimated by a slit-lens assembly taken from an XL-A AUC containing only one 10 mm lens and passed the 25 μm slit which defines the radial resolution of the system. Then it was finally coupled into a 1000 μm optical fiber, which transported the light to a CCD array spectrometer. The whole optics in the vacuum chamber was fixed to an arm, which allowed for radial scanning of the AUC cell. The data acquired using this system clearly showed what was possible by adding a spectral dimension to AUC; however it also suffered from a number of problems (Bhattacharyya 2006). First of all, this MWL system produced noisy spectra, which prevented further hydrodynamic analysis. In addition, the intensity was very low in the UV region.

To overcome some of these limitations, the design was modified in how light was focused into the detection fiber (Fig. 5.2 right, elements 4–6; a photo of this setup

[2]Note that the light can only be made parallel for one wavelength due to the wavelength dependence of the refractive index (chromatic aberration).

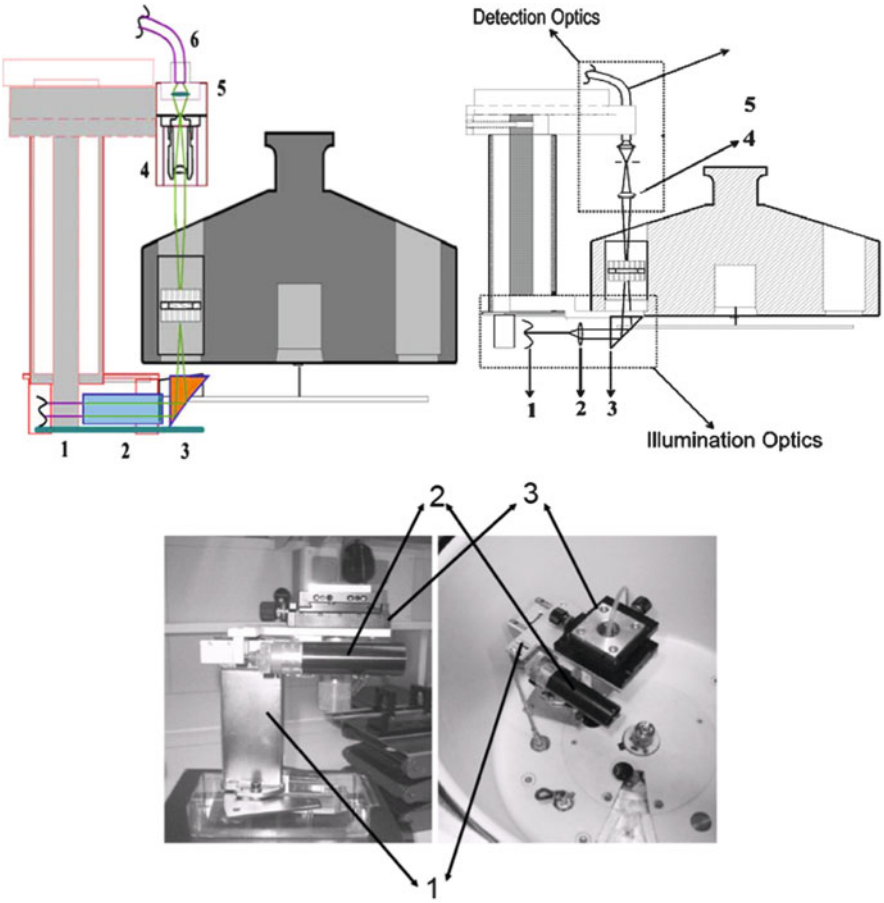

Fig. 5.2 First-generation MWL detectors
Left: Very first experimental MWL optics setup. (*1*) 600 μm patch fiber, UV/Vis (Ocean optics). (*2*) The collimating lens system (self-built) $f = 20.6$ mm biconvex. (*3*) 90 °quartz prism. (*4*) Slit-lens assembly (from the XL-A) only one lens $f = 10$ mm biconvex. (*5*) Focusing (OZ Optics) $f = 15$ mm. 6–1000 μm patch fiber, UV-Vis (Ocean Optics). *Right*: Modified detector arm. The detector arm. 1, 2, and 3 are the same as in the earlier setup. (*4*) Biconvex lens $f = 20$ mm. (*5*) Slit of dimension 25 μm. (*6*) Biconvex lens $f = 10$ mm (*7*) 600 μm patch fiber (Ocean optics). The light path is also shown schematically. *Lower*: Photograph of the arm. (*1*) Detector arm, (*2*) stepping motor (0.1 μm resolution at up to 4 mm/s), (*3*) detection unit with X-Y positioning screws. Right: Mounted arm in the AUC chamber (Images taken from Bhattacharyya (2006) with permission)

is shown in Fig. 5.2 lower panel). (Bhattacharyya 2006; Bhattacharyya et al. 2006). This setup improved the intensity in the UV region and decreased the noise some. Furthermore, the system became more stable (Bhattacharyya 2006).

5.3.2 Second-Generation MWL Detectors

The second-generation detector design was significantly improved concerning light intensity and optical quality, since the light after the cell was not anymore coupled into a fiber after passing a 25 μm slit for the optical resolution (Fig. 5.2) and then passed another 25 um slit at the spectrometer entrance for the wavelength resolution, but now the spectrometer was directly mounted on the detector arm (Figs. 5.3 and 5.4) (Karabudak 2009). This eliminated one slit in the optical path, which significantly improved the light intensity as now the 25 μm slit of the spectrometer is simultaneously used for the definition of the radial as well as of the spectrometer wavelength resolution. This is the open AUC second-generation detector design (downloadable for free using the open AUC website (http://wiki.bcf2.uthscsa.edu/openAUC/wiki/WikiStart)), which is in use since 2008 up to now and which since then has been further improved by gradual changes. The most notable of them are (1) the programming of a new control and data acquisition software by Johannes Walter based on Labview and 64 bit technology (Walter et al. 2014), which eliminated the occasional timing problems of the first MWL generation 32 bit MWL control and data acquisition software (Karabudak 2009; Bhattacharyya 2006; Bhattacharyya et al. 2006), and (2) the alternative development of an external hardware solution, which takes over all time critical multiplexing steps by Nanolytics (Pearson et al. 2015).

The second-generation optical system uses a high-power Xe flash lamp L-9456-12 from Hamamatsu Photonics GmbH, which has a flash rate of 530 Hz. This is

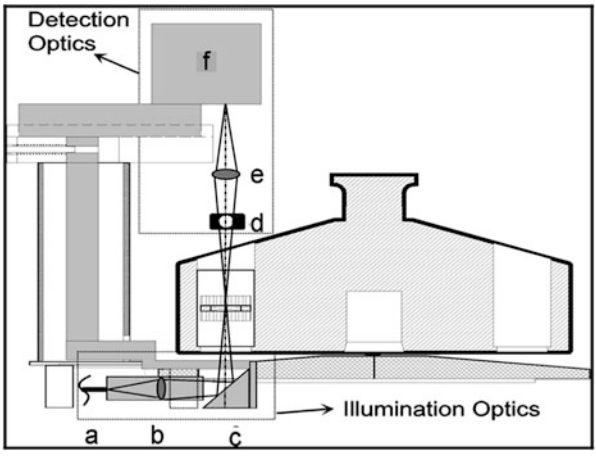

Fig. 5.3 Schematics of the second-generation MWL detector arm (Taken from Karabudak (2009) with permission) (**a**) 600 μm patch fiber UV/Vis (Ocean Optics). (**b**) The collimating lens system (self-built), $f = 20.6$ mm biconvex. (**c**) 90° quartz prism. (**d**) Iris diaphragm for reducing light intensity. (**e**) Focusing biconvex lens (40 mm). (**f**) Spectrometer. The light path is also shown schematically

about five times faster than that of the Beckman Coulter XL-A allowing for faster flashing which increases the detection speed. The light from the lamp is passed from the fiber (Fig. 5.3a) through a collimating lens (Fig. 5.3b). The (almost) parallel light is then reflected by a 90° mirror (Fig. 5.3c). Afterward, the light passes the sample compartment and reaches an adjustable iris (Fig. 5.3d). The iris is used for adjusting the total intensity since the light in the visible is so intense that it maxes out the spectrometer, while that in the UV is significantly reduced as compared to the initial white light spectrum from the flash lamp. Finally light reaches a collimating lens, which images the cell and focuses the light into the 25 μm entrance slit of the Ocean Optics USB2000 spectrometer. The USB2000 spectrometer uses CCD technology, which has one fixed wavelength for each of the pixels. These pixels can be read out in a few milliseconds, yielding 2000 data points, which allows for averaging the data from several pixels at each wavelength. Newer spectrometers have 3000 pixel CCD chips.

5.3.3 *Mechanical Parts of Second-Generation MWL-AUC*

There are two main mechanical parts of the open AUC MWL-AUC (Strauss et al. 2008). Firstly, the detector arm is the main mechanical part of MWL-AUC as shown in Fig. 5.4. This arm carries the spectrometer, the stepping motor, lenses, iris, and quartz prism. The second mechanical part of MWL-AUC is the vacuum feedthrough. The vacuum feedthrough includes the electronic feedthrough and optical feedthrough. The electronic feedthrough is used for the USB signal from

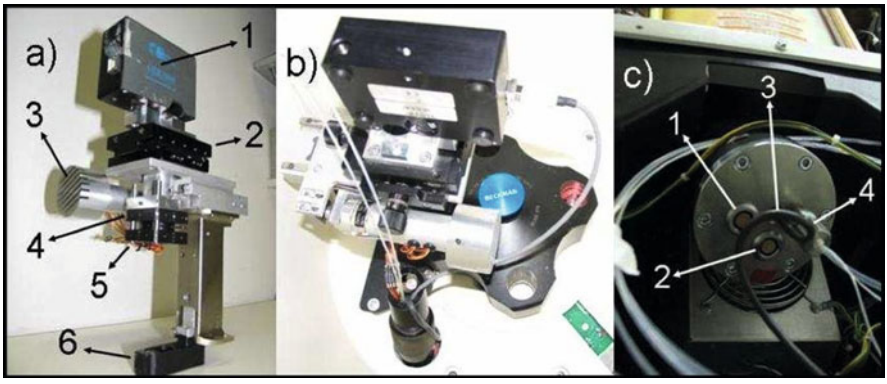

Fig. 5.4 Photographs of second-generation MWL-AUC (Taken from (Karabudak 2009) with permission).(**a**) Photograph of the detector arm: *1* spectrometer. *2* table with the possibility of X-Y movement. *3* step motor. *4* lens (40 mm biconvex). *5* iris *6* 90° quartz prism. (**b**) The arm fitted in the centrifuge. (**c**) Photograph of the vacuum feedthrough: *1* Electronic feedthrough for step motor. *2* Electronic feedthrough for spectrometer. *3* Electronic connection for TTL pulse for rpm measurements. *4* Optical feedthrough for fibers

and to the spectrometer, step motor, and Transistor-Transistor Logics (TTL) pulses for speed measurements. The optical feedthrough is used for fiber connections. All these mechanical parts are mounted into a preparative ultracentrifuge. In order to mount the feedthrough into the preparative machine, the heat sink of the preparative machine needs to be modified. This requires drilling holes into the heat sink of the preparative ultracentrifuge as shown and discussed in the open AUC publication (Coelfen et al. 2010) and the user loses the Beckman Coulter warranty. A more elegant solution is to take an XL-A heat sink and then use the hole for the flash lamp to plug in the vacuum feedthrough as shown in Fig. 5.4c. This allows maximum flexibility and more importantly allows the modification of any XL-A AUC into a MWL-AUC and back again in about an hour. To accommodate swapping, a slit was cut into the thermal shroud to allow mounting of the detector arm.

5.3.4 Electronics of MWL-AUC

There are four main electronic parts of MWL-AUC. First, an optical sensor is used to time the rotor revolution over speeds ranging from 1000 rpm to 60,000 rpm. A TTL timing pulse generated by light reflected from a spot on the rotor allows measurement of this speed and even allows the system to follow steep speed ramps for very polydisperse samples (Mächtle 1999; Bhattacharyya et al. 2006). The speed is measured by a national instrument digital counter/timer card. This card measures the TTL pulse for speed determination and triggers the flash lamp and spectrometer when the cell of interest passes the optical path. Second, there is a USB connection for the USB spectrometer. This connection collects the spectral data and sends it to the computer. A computer is used to control the digital counter/timer card, USB connector, and data collection. The third electronic part is the USB spectrometer. This spectrometer is triggered by the counter card and sends the digital signal to the computer via the USB connection. The fourth part is the stepping motor, which is controlled by the MWL-AUC control software. As soon as data are taken at a given radial position, this motor moves the detector arm to the next radial position at the radial specified step interval.

5.3.5 Software of MWL-AUC

Initially, the MWL detector was programmed using Labview programming language in a 32 bit version. The Labview control program was controlling the timer/counter card as well as the movement of the step motor. In addition, the software triggers the flash lamp and spectrometer and collects the data from the spectrometer. The software also calculates the absorption and plots it. Furthermore, the software stores the data on the computer hard disk. The initial program allowed for radial scanning at constant speed and for speed ramps but suffered from occasional timing problems

of the trigger pulses. This was overcome with the 64 bit program (Walter et al. 2014) as well as the omega device (Pearson et al. 2015).

5.4 MWL-AUC in the Scientific Literature

Although the first publication about the MWL detector (first generation) was published in 2006 (Bhattacharyya et al. 2006), nine years before the time of writing of the present manuscript, not many publications have appeared using the MWL-AUC. The reason for this is that the MWL detector was only available in a few dedicated laboratories and was still under continuous development. Additionally, data evaluation by powerful evaluation packages like the UltraScan (Gorbet et al. 2015) or Sedanal (Walter et al. 2015) became available only very recently. The situation has, therefore, now improved. The MWL detector has a quality comparable or superior to the Beckman Coulter XL-A in the visible and even in the UV (Walter et al. 2014; Strauss et al. 2008; Gorbet et al. 2015) and is freely available from the open AUC website (http://wiki.bcf2.uthscsa.edu/openAUC/wiki/WikiStart). In addition, it can be reversibly mounted into any XL-A AUC (after cutting of a slit into the can for the detector arm). These improvements will very likely lead to more operational MWL detectors. In addition, the CFA will soon be available, which will have a third-generation MWL detector installed (Laue and Austin in press).

While the first publication described the basic MWL design and first measurements, it already contains first measurements, which qualify the MWL as multi-sensitivity turbidity detector due to the proportionality of the scattering intensity with the particle radius to the power of six and the wavelength of light to the inverse power of four (Bhattacharyya et al. 2006). Large particles scatter light a lot and can be detected at higher wavelengths than the weaker scattering small particles, which can be detected at short wavelengths with higher sensitivity. Due to the spectral dimension, an optimum wavelength can be found for each particle size, which significantly enhances the dynamic range of turbidity detection

Strauss et al. analyzed the first prototype of the second-generation MWL-AUC (Strauss et al. 2008). The performance of the optical setup MWL-AUC was tested, and the result was compared with the commercial XL-A showing that MWL wavelength accuracy and radial resolution are comparable with the XL-A. In addition wavelength dependent noise levels were compared and showed that the MWL was better than the XL-A in the visible range and worse in the UV as a result of UV light attenuation by the optical fiber. This publication is important because it showed for the first time that MWL-AUC is comparable with the commercial detector but has the advantage of adding the spectral dimension to the data. The advantage of this spectral dimension becomes obvious already in the raw data. Figure 5.5 shows a sedimentation experiment of an industrial and commercial product with MWL-AUC (Karabudak et al. 2010a). The product is gelatin-coated β-carotene composite particles, which are industrially used as food colorants.

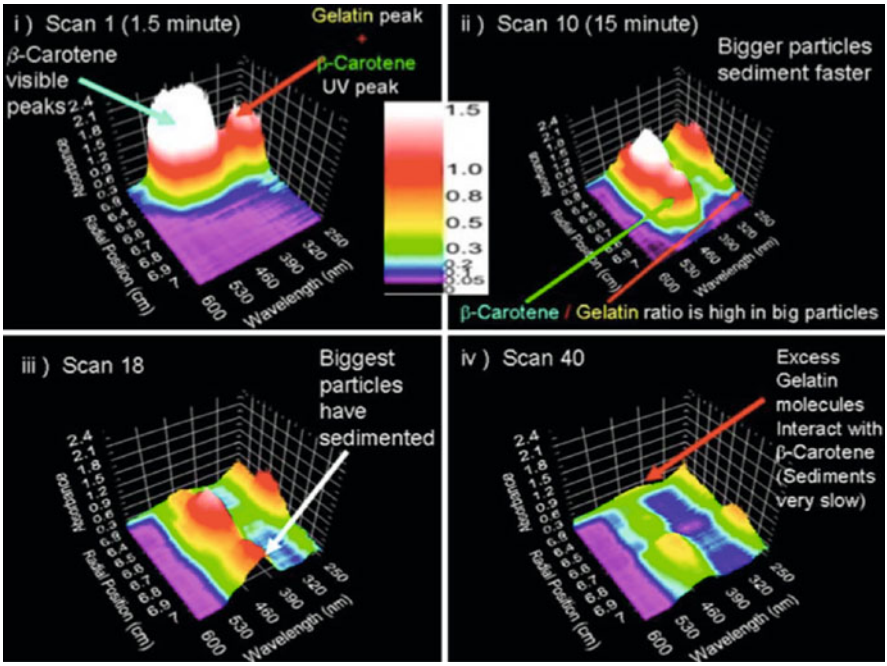

Fig. 5.5 Three-dimensional plots of the raw data from a band sedimentation experiment with β-carotene detected with the MWL detector (Taken from Karabudak et al. (2010a) with permission)

The raw data from this experiment in Fig. 5.5 show that the product contains multiple species as labeled. Carotene absorbs in the visible around 460 nm and gelatin in the UV at 280 nm. The fastest-sedimenting species mainly consists of carotene, while the second fastest species contains carotene and significantly more gelatin than the fastest-sedimenting species. Finally free gelatin and gelatin interacting with β-carotene sediment slowly. Not only could the raw data show the number and spectral characteristics of the components. Spectral analysis of the fractionated species showed that the previously assumed structure of the product was not correct. MWL-AUC showed that H-aggregates and J-aggregates are formed in different species and that a previously published literature structure (Auweter et al. 1999) is not correct.

In another study, scientists extensively studied the interaction of single-walled carbon nanotubes (SWCNTs) with surfactants (Backes et al. 2010a) and determined the surfactant density of SWCNTs. Also surfactants were tested for SWCNT absorption (Backes et al. 2010a). This kind of study is not possible with the commercial XL-A, since each of the SWCNT species has its spectral fingerprint. Therefore, simultaneous fractionation and size determination as well as spectral detection for each of the fractionated species are necessary.

When a carbon nanotube, surfactant, and intercalant system were analyzed by MWL-AUC (Karabudak et al. 2010b), the results showed that previously published

results on this system were incorrect (Backes et al. 2010b). The MWL-AUC experiments revealed that the intercalant is oxidized and sediments independent of the carbon nanotubes. This finding changed the previously assumed function of the intercalant.

In a recent study, Walter et al. (2014) studied polydisperse nanoparticles successfully. An impressive example was the MWL experiment on Au nanoparticles, which shows size- and shape-dependent UV/Vis spectra due to the surface plasmon resonance. Polydisperse Au nanorods (Fig. 5.6a) were subjected to MWL-AUC. The

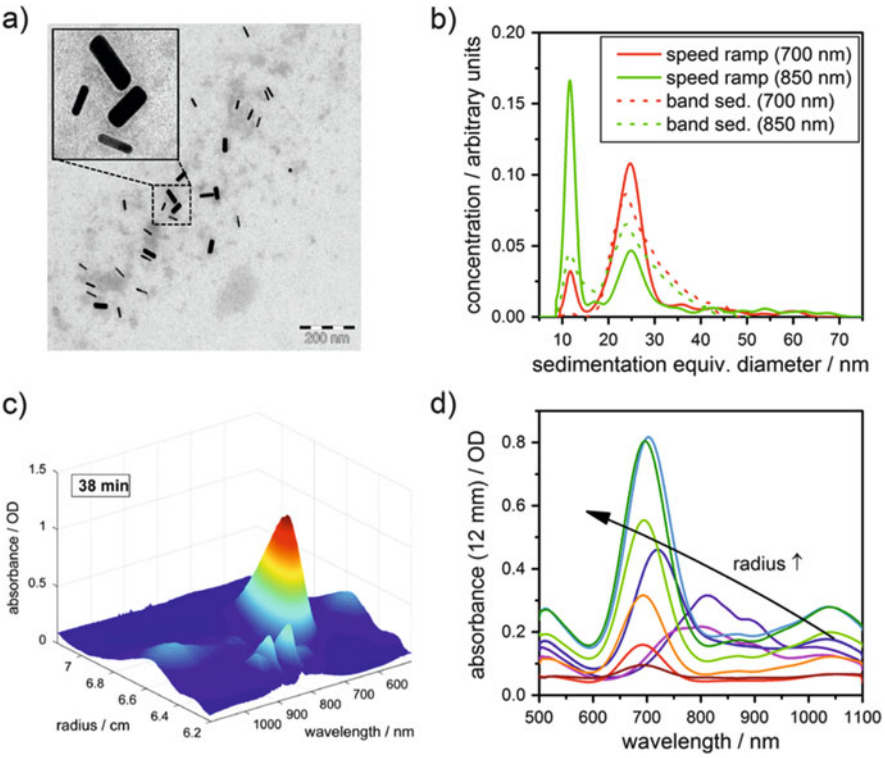

Fig. 5.6 (**a**) TEM image of a gold nanorod mixture clearly showing the two main species. (**b**) Extinction weighted particle size distribution of two mixtures of the same nanorod species gained at a speed ramp and band sedimentation experiment evaluated at 700 and 850 nm. (**c**) Multiwavelength spectra of gold nanorods sedimenting at 2 krpm in a direct band centrifugation experiment as a function of the radial distance from the axis of rotation for a scan taken after 38 min. The three-dimensional data surface is clearly visible. (**d**) Absorbance data of gold nanorods recorded in the radial dimension from 6.3 to 7.1 cm with 1 mm increment (*purple* to *blue* to *green* to *red* and *arrow* as a guide to the eyes) for the same snapshot (**c**) after 38 min in the band centrifugation experiment. A higher radial position results in an increased sedimentation equivalent diameter, which causes a redshift in the absorption spectrum due to the particle size- and shape-dependent surface plasmon resonance (Taken from Walter et al. (2014) with permission)

particle size distributions (Fig. 5.6b) showed wavelength-dependent differences in the intensity, which is expected from the size-dependent UV/Vis spectra.

A scan containing raw data (Fig. 5.6c) shows the complexity of the three-dimensional data surface and directly allows to reveal the spectral properties of the different species in the mixture. From this complex three-dimensional surface, the spectra at different radii can be extracted and show the change of the UV/Vis spectra with location and size of the nanoparticles. Due to these advantageous properties, MWL-AUC was applied for other complex mixtures like polyfluorene-coated semiconductor particles (de Roo et al. 2014).

A very recent report showed that application of the Sedanal software to multiwavelength data allows for an easy and successful deconvolution of individual spectra of components in a mixture (Fig. 5.7) (Walter et al. 2015). In this example, blue silica nanoparticles were mixed with Au nanoparticles. The spectra are shown in Fig. 5.7a. MWL-AUC (Fig. 5.7b) shows that two different components can be seen with distinctly different spectra. Deconvolution of the mixture spectra yields the spectra of the individual components in good quality (Fig. 5.7d), and the sedimentation coefficient distributions of the individual components could also be deconvoluted (Fig. 5.7c). The wiggle in the sedimentation coefficient distribution is an as yet unexplained artifact.

Another exciting and recently reported application is the use of MWL-AUC to detect spectra of nucleating species (Voelkle et al. 2015). Overlaying the two reactants of a crystallizing species in an AUC cell by the technique of synthetic boundary crystallization ultracentrifugation (Borger et al. 2000) allows to initiate the reaction in a sharp boundary formed upon speeding up the ultracentrifuge. Since one reactant is consumed within seconds, further nucleation and growth are quenched and the formed early nucleation and growth species get then fractionated by the ultracentrifugal field and can then be detected. Since the particle size resolution of the AUC is in the Angström range for such small species (Colfen and Pauck 1997), valuable information about the early species in a crystallization reaction can be obtained. Addition of the spectral dimension by MWL-AUC now significantly increases the information content by the UV/Vis spectra of the different species. An example for Ag nucleation was recently reported (Voelkle et al. 2015).

The last and most recent example discussed in this MWL overview is the application of MWL-AUC for biopolymer samples, which is certainly one of the most important applications for AUC. MWL-AUCs using detectors of the second generation have the problem of UV attenuation as discussed above, which significantly decreases the data quality in this important wavelength range. Nevertheless, a recent study on BSA-DNA mixtures shows that proteins can be investigated by MWL-AUC as well, yielding unsurpassed information, which cannot be obtained with the XL-A ultracentrifuge as a direct comparison of MWL and XL-A data showed (Pearson et al. 2015; Gorbet et al. 2015). Figure 5.8 shows the raw data for the BSA mixture with two different DNA fragments.

From these data, already three species can be identified. The fastest-sedimenting species coded with yellow in Scan 10 and 25 with absorption around 260 nm is likely a DNA species. A second following species absorbs broadly from 240 to

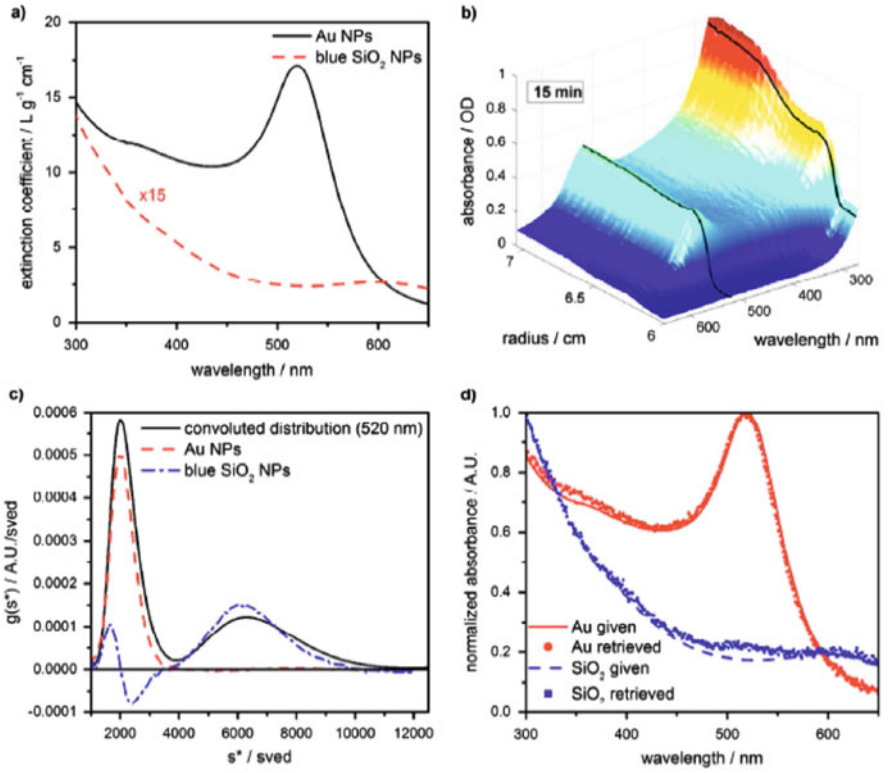

Fig. 5.7 (**a**) Extinction coefficients of the silica and gold NPs. The extinction coefficient of the silica NPs was multiplied by 15 to be better recognizable. (**b**) Multiwavelength spectra of the silica-gold mixture sedimenting at 4 krpm in a sedimentation velocity experiment as a function of the radial distance from the axis of rotation. The scan was taken after 15 min. Two different wavelengths corresponding to the spectral features of the two species were highlighted with black lines as a guide to the eye. (**c**) Convoluted sedimentation coefficient distributions at 520 nm and deconvoluted sedimentation coefficient distributions of gold and silica NPs. 329 wavelengths values were used for the MWL analysis. The distributions were not normalized for the sake of clarity. (**d**) Extinction spectra of the two species measured using a benchtop UV/Vis spectrometer as well as the extinction data reproduced from the MWL-AUC experiment. Spectra were normalized to a maximum value of one to be comparable (Taken from Walter et al. (2015) with permission)

280 and thus likely contains protein and DNA and the same is true for the slowest-sedimenting species in Fig. 5.8.

Evaluation of this experiment with UltraScan 3.0, which is now able to fully analyze MWL data, reveals much more detail about the sample mixture.

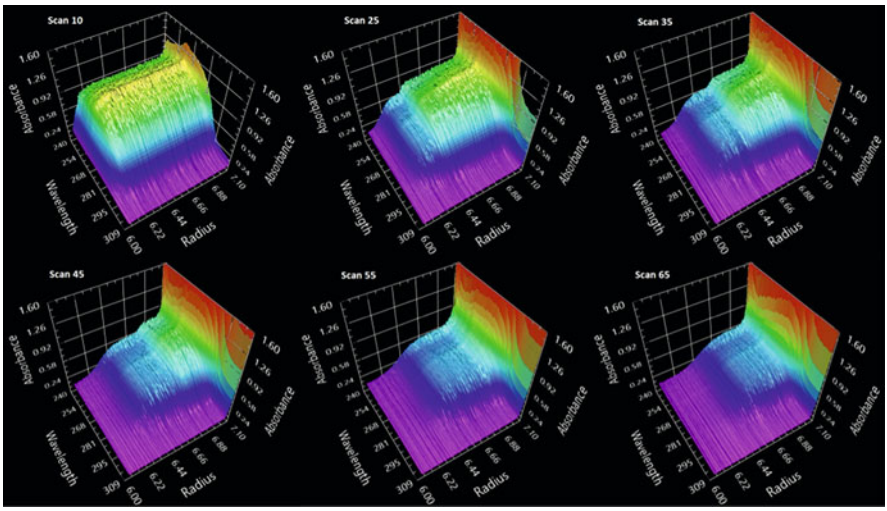

Fig. 5.8 Time series images of three-dimensional sedimentation absorbance data for a DNA-BSA mixture from open-source MWL recorded with 50 μm radial step size. The intensity in OD units is dependent on the extinction coefficient at each wavelength. The absorbance spectra of the species in solution are evident across the wavelength range. The *yellow* coded species at ca. 270 nm across the spectra is indicative of a more rapidly sedimenting species, in this case a larger DNA fragment (Image reproduced from Pearson et al. (2015) with permission)

Two-dimensional spectrum analysis (2DSA) shows BSA monomers and dimers as well as a 208 base pair DNA sedimenting at almost the same speed like the BSA. Only the additional spectral dimension makes it possible to distinguish these almost equally fast-sedimenting species. The faster sedimenting 12 S species turned out to be 2811 base pair DNA and the fastest-sedimenting species at low concentration were uncut DNA plasmids. This example shows in an impressive way what can be learned from MWL-AUC experiments with a sophisticated analysis as is possible with UltraScan (Fig. 5.9).

Other analysis methods implemented into UltraScan are also possible with MWL data, which was demonstrated for the van Holde-Weischet method, which is especially attractive since it needs no assumptions about the sample (Gorbet et al. 2015).

If the UV/Vis spectra of the individual components in the mixture are known, like in this case those for BSA and DNA, it is possible to deconvolute the MWL data of mixtures of these components into the contributions of each component to the detected mixture UV/Vis spectrum. It is then possible to average the individual sedimentation velocity profiles of each component in the mixture for each

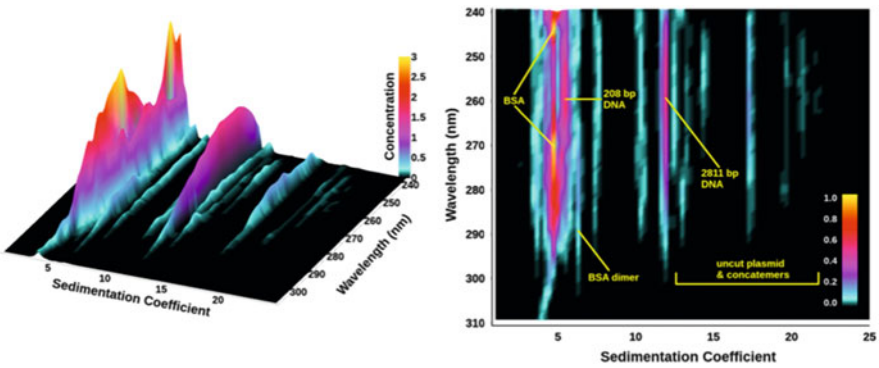

Fig. 5.9 *Left:* Three-dimensional view of the sedimentation profile as a function of wavelength for a 50:50 DNA-BSA mixture. The protein absorbance spectrum at 4.3 s (*two yellow peaks*) can be clearly distinguished from the DNA peak with absorbance maximum around 258 nm. Minor species can be identified based on their spectrum. *Right:* Projection view of the 2DSA-MC sedimentation profile as a function of wavelength for the 50:50 DNA-BSA mixture. Remarkably, the protein absorbance spectrum at 4.3 s (*two yellow peaks*) can be clearly distinguished from the adjacent DNA peak with absorbance maximum around 258 nm, despite the proximity of the peaks (4.5 s vs. 5.2 s). Minor species can be identified based on their spectrum. The *straight lines* attest to the high resolution and robustness of this approach to fit multiwavelength data (each wavelength is separately analyzed) (Taken from Gorbet et al. (2015) with permission)

wavelength according to the wavelength-dependent extinction coefficient profile and arrive at two spectrally decomposed sedimentation velocity profiles for BSA and DNA individually (Gorbet et al. 2015). This spectral decomposition works extremely well as was demonstrated for different BSA-DNA mixing ratios. If now the sedimentation velocity profiles are evaluated for the two components, the data in Fig. 5.10 are obtained.

Figure 5.10 shows that the individual sedimentation coefficient distributions are obtained for DNA as well as for BSA in a very high quality showing all species present in the mixture. For the XL-A, such high-quality analysis is not possible (Fig. 5.10). In addition the MWL decomposition showing the sedimentation coefficient plotted versus the shape in terms of the frictional ratio reveals the sedimentation coefficients of the individual species in the complex mixture together with their frictional ratio/shape. The XL-A analysis, even when performed for the two relevant wavelengths, lacks this resolution clearly showing the advantage of the spectral dimension in the MWL-data.

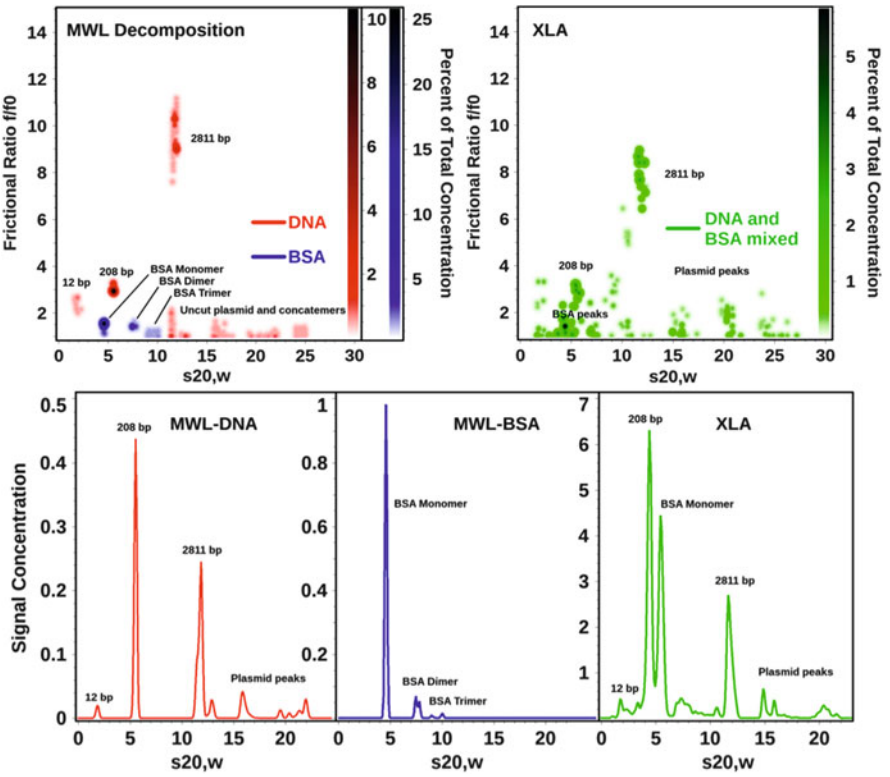

Fig. 5.10 Global genetic algorithm Monte Carlo analysis of decomposition results obtained from six different DNA and BSA mixtures analyzed on the open AUC MWL instrument (*top left*) and the dual wavelength results obtained from the Beckman Coulter XL-A (*right panel*). The separate decomposition results for DNA (*red*) and BSA (*blue*) are combined in the left panel pseudo-three-dimensional plot to illustrate the exceptional separation achieved by spectral decomposition which even separates species with nearly identical sedimentation coefficients (the two major species sedimenting near 5 S). This approach demonstrates the superior resolution obtained from MWL analysis compared to the global 2-wavelength analysis performed on the Beckman Coulter XL-A (*right panel*, *green*). Lower panel: differential distributions from the same data shown above (*red*, decomposition for DNA; *blue*, decomposition for BSA; *green*, non-separated XLA data for DNA-BSA mixtures globally fitted to genetic algorithm – Monte Carlo analysis) (Taken from Gorbet et al. (2015) with permission)

5.5 Conclusions

In this chapter, we discussed the development as well as design and applications of the MWL detector. This detector has a huge advantage over existing AUC detectors by the addition of a spectral dimension to the hydrodynamic data from AUC. MWL-AUC has now reached a data quality, which allows its application for the wide range of samples from (bio)polymers to nanoparticles with a data quality comparable or

superior to that of the Beckman Coulter XL-I instrument. Fiber solarization is still an issue in the second-generation MWL detectors, although it could be demonstrated that even with attenuated UV intensity, a high-quality analysis of biological samples is possible (Gorbet et al. 2015). Already the MWL raw data contain a significant amount of information. This information content can be dramatically increased if sophisticated data analysis packages like UltraScan or Sedanal are used, which were recently adapted for the analysis of MWL data. Therefore, everything necessary for the successful application of MWL-AUC is now available. The second-generation open AUC detector construction plans can be freely downloaded from the open AUC website (http://wiki.bcf2.uthscsa.edu/openAUC/wiki/WikiStart). This detector can be mounted in any XL-A after introduction of a cut for the detector arm in the can and can be reversibly exchanged with the XL-A optics. Importantly, the new CFA AUC will have a third-generation (Laue and Austin in press) MWL detector, which works with mirror optics and thus avoids the light attenuation in the UV in the optical fibers as well as chromatic aberration problems. The data quality of this detector will be superior to the fiber-based MWL designs. For all these reasons, a wide use of MWL-AUC can be expected in the near future. Although only a few publications using MWL-AUC exist so far, they all demonstrate the superior information content of these measurements by the added spectral dimension. Therefore, we expect that this detector will enable measurements, which have so far not been possible by AUC, and that MWL-AUC will help to solve important scientific problems in the future.

Acknowledgments We thank a number of people who helped to make MWL-AUC what it is today. First of all, we acknowledge funding of the AUC 2004 project by BASF SE, which made the start of this project possible. Dr. Walter Mächtle, Dr. Lars Börger, and Dr. Wendel Wohlleben, all from BASF SE, are thanked for the fruitful cooperation over the years of development. Dipl. Ing. Johannes Walter (University of Erlangen) is thanked for the new data acquisition software. We also thank Dr. Kristian Schilling (Nanolytics) for discussions and exchange of ideas during detector development. Prof. Dr. Borries Demeler (University of Texas, Health Center, at San Antonio) is thanked for adapting the UltraScan evaluation software to MWL data, which now allows unsurpassed evaluations using MWL-AUC as well as for a long-standing cooperation in this area. We also thank all students and coworkers who worked and work in the Cölfen lab on MWL development, namely, Patricyja Maciejewska, Saroj Bhattacharyya, Akif Gülsün, Basri Cicek, Dirk Haffke, Joe Pearson, Dr. Holger Strauss, and Dr. Karel Planken.

References

Auweter H et al (1999) Supramolecular structure of precipitated nanosize beta-carotene particles. Angew Chem Int Ed 38:2188–2191. doi:10.1002/(sici)1521-3773(19990802)38:15<2188::aid-anie2188>3.0.co;2-#

Backes C et al (2010a) Determination of the surfactant density on SWCNTs by analytical ultracentrifugation. Chem Eur J 16:13176–13184. doi:10.1002/chem.200903461

Backes C et al (2010b) Nanotube surfactant design: the versatility of water-soluble perylene bisimides. Adv Mater 22:788–802. doi:10.1002/adma.200902525

Bhattacharyya SK (2006) Development of detectors for the analytical ultracentrifuge, PhD thesis, Universität Potsdam

Bhattacharyya SK et al (2006) Progress in colloid and polymer science: analytical ultracentrifugation VIII, Springer, pp 9–22

Borger L, Colfen H, Antonietti M (2000) Synthetic boundary crystallization ultracentrifugation: a new method for the observation of nucleation and growth of inorganic colloids and the determination of stabilizer efficiencies. Colloids Surf A Physicochem Eng Asp 163:29–38. doi:10.1016/s0927-7757(99)00427-6

Coelfen H et al (2010) The open AUC project. Eur Biophys J Biophys Lett 39:347–359. doi:10.1007/s00249-009-0438-9

Colfen H, Pauck T (1997) Determination of particle size distributions with angstrom resolution. Colloid Polym Sci 275:175–180. doi:10.1007/s003960050068

de Roo T et al (2014) A direct approach to organic/inorganic semiconductor hybrid particles via functionalized polyfluorene ligands. Adv Funct Mater 24:2714–2719. doi:10.1002/adfm.201304036

Giebeler R (1992) In: Harding SE, Rowe AJ, Horton JC (eds) Analytical ultracentrifugation in biochemistry and polymer science. Royal Society of Chemistry, Cambridge, pp 16–31

Gorbet G, Pearson J, Demeler A, Cölfen H, Demeler B (2015) Next generation AUC (2): multi-wavelength data analysis adds a spectral dimension to hydrodynamic information. Methods Enzymol 562:27–47

http://wiki.bcf2.uthscsa.edu/openAUC/wiki/WikiStart

Karabudak E (2009) PhD thesis; Development of MWL-AUC / CCD-C-AUC / SLS-AUC detectors for the analytical ultracentrifuge PhD thesis, Max Planck Institute of Colloids and Interfaces

Karabudak E, Wohlleben W, Colfen H (2010a) Investigation of beta-carotene-gelatin composite particles with a multiwavelength UV/vis detector for the analytical ultracentrifuge. Eur Biophys J Biophys Lett 39:397–403. doi:10.1007/s00249-009-0412-6

Karabudak E et al (2010b) A universal ultracentrifuge spectrometer visualizes CNT-intercalant-surfactant complexes. ChemPhysChem 11:3224–3227. doi:10.1002/cphc.201000504

Laue T, Austin B (in press) The CFA analytical ultracentrifuge architecture. Analytical ultracentrifugation: instrumentation software and application

MacGregor IK, Anderson AL, Laue TM (2004) Fluorescence detection for the XLI analytical ultracentrifuge. Biophys Chem 108:165–185. doi:10.1016/J.Bpc.2003.10.018

Mächtle W (1999) High-resolution, submicron particle size distribution analysis using gravitational-sweep sedimentation. Biophys J 76:1080–1091

Müller H (1989) Automated determination of particle-size distributions of dispersions by analytical ultracentrifugation. Colloid Polym Sci 267:1113–1116

Pearson J et al (2015) Next generation AUC (1): multi-wavelength detectors for the analytical ultracentrifuge add a spectral dimension to AUC instrumentation. Methods Enzymol 562:q–26

Strauss HM et al (2008) Performance of a fast fiber based UV/Vis multiwavelength detector for the analytical ultracentrifuge. Colloid Polym Sci 286:121–128. doi:10.1007/s00396-007-1815-5

Voelkle C, Gebauer D, Cölfen H (2015) High-resolution insights into the early stages of silver nucleation and growth. Faraday Discuss 179:59–77. doi:10.1039/C4FD00269E

Walter J et al (2014) Multidimensional analysis of nanoparticles with highly disperse properties using multiwavelength analytical ultracentrifugation. ACS Nano 8:8871–8886. doi:10.1021/nn503205k

Walter J et al (2015) Simultaneous analysis of hydrodynamic and optical properties using analytical ultracentrifugation equipped with multiwavelength detection. Anal Chem 87:3396–3403